

Combined smoothing method and its use in combining Earth orientation parameters measured by space techniques

J. Vondrák¹ and A. Čepek²

¹ Astronomical Institute, Academy of Sciences of the Czech Republic, Boční II, 141 31 Prague 4, Czech Republic
e-mail: vondrak@ig.cas.cz

² Faculty of Civil Engineering, Czech Technical University, Thákurova 7, 166 29 Prague 6, Czech Republic
e-mail: cepek@fsv.cvut.cz

Received March 13; accepted August 31, 2000

Abstract. The new combined method of smoothing observational data, being a generalization of the Whittaker-Robinson-Vondrák method based on probability, is designed. Its objective is to remove the high-frequency noise present in the observations of an (analytically unknown) time function and its first derivatives. The method consists in finding a weighted compromise among three different conditions: smoothness of the searched curve, its fidelity to the observed function values and its fidelity to the observed first time derivatives. The method assumes that the observations are distributed non-uniformly, with different uncertainties, and that the epochs of both input series containing the observed function values and first derivatives are not identical. Its possibilities are demonstrated on combining both simulated data and the Earth orientation parameters observed by different space techniques: Very Long Baseline Interferometry and Global Positioning System, namely the Universal Time/length of day changes and polar motion/polar motion rate.

Key words: methods: numerical — techniques: miscellaneous — reference systems

1. Introduction

The method based on the original Whittaker-Robinson (1946) method of smoothing observational data was described by Vondrák (1969, 1977) in order to suppress high-frequency noise present in the observations. The method uses unequally spaced input data of different uncertainties of measurement to derive a set of points lying on a smooth

curve. The basic idea consists in finding a compromise between “fidelity” of the searched smooth curve to the observed values on the one hand, and the “smoothness” of the curve on the other. The method became quite popular in many branches of astronomy; e.g., it is routinely used at the International Earth Rotation Service (IERS) to obtain smooth curves of the Earth Orientation Parameters (EOP), in atomic scale smoothing (Guinot 1988) or in analyses in stellar astronomy (Harmanec et al. 1978; Štefl 1995). The method, whose properties were studied in detail by Feissel & Lewandowski (1984), is further referred to as “original smoothing”.

However, we are very often facing a more general problem when not only the values of the function itself but also its first time derivatives are measured. Quite often, the former is given with larger spacing, and the latter, with a higher time resolution, is then used to make the output series denser. The analytical expression of the measured function is generally unknown, but we can assume that it is continuous and relatively smooth. This occurs, e.g., when the values of Universal Time UT1 (defined by the rotation of the Earth) are measured by Very Long-Baseline Interferometry (VLBI), and at the same time the variations in length of day (l.o.d.) are measured by Global Positioning System (GPS). The former represents the angle between zero meridian and a fiducial point on the celestial sphere, whose value is a non-linear function of time, while the latter is its change during one day. Another example is polar motion that is determined by GPS, and the same technique yields simultaneously also its rate.

Of course, the same estimator can be applied to both series separately and independently, but in such a case the result would be two functions, mutually not fully consistent – the latter would not be exactly the time derivative of the former. Using this approach in practical application would lead to unsatisfactory results, namely in case when less frequent VLBI determinations of UT1 and more

frequent GPS determinations of l.o.d. are treated. In this specific case, the separate smoothing of UT1 from VLBI would lack the variations with short periods, and separate smoothing of l.o.d. would suffer from long-periodic instabilities. In order to remove these instabilities, present practice of GPS analysis is to “scale” the values of l.o.d. against VLBI determination of UT1 on intervals several weeks long.

Here we propose a more general method of smoothing in which the estimation is done from all available data obtained by both techniques of observation. Both data series are combined to yield two smooth curves tied by the constraints assuring that the latter is the time derivative of the former. The first one fits well to the first data series and the second one fits well to the second series. This approach also provides an important test of systematic errors specific for each of the data series that are difficult to reveal had both series be treated separately. The goal is to make use of advantages of both series (long-term stability of the former and higher time resolution of the latter) in one solution. The main ideas of the method are shortly outlined and its use in combining the VLBI and GPS data is demonstrated by Vondrák & Gambis (2000); here we describe the method in a greater detail, and give more examples of application.

2. Combined smoothing

In general, two time series of observations are available – one with measured function values of a certain quantity whose analytic expression is unknown (Series 1) and the other with measured time derivatives of the same quantity (Series 2). Both series are given at unequally spaced epochs that need not be necessarily identical, and the individual observations are given with different precision, defined by their formal uncertainties (that can be easily converted into weights). We further assume that both series are independent one from the other, and also that the individual observations of the same series are de-correlated. The situation is illustrated in Fig. 1, where the upper plot shows the observed function values and their uncertainties (Series 1), the lower plot depicts Series 2 with the observed values of the first derivatives with their uncertainties. Full lines in both plots represent the smoothed values; the lower one is the first derivative of the upper one.

2.1. Theoretical basis

We are looking for a unique time series defined at all points with observations (no matter whether belonging to Series 1 or 2), lying on a sufficiently smooth curve, whose function values fit well to the values of Series 1 and whose

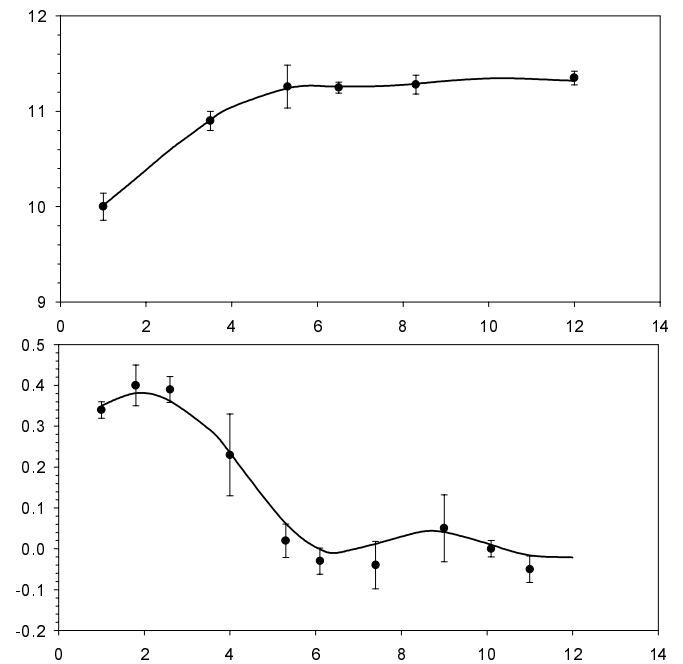


Fig. 1. Illustration of combined smoothing. Full circles and vertical lines represent the observations and their uncertainties, full lines the smoothed curves (top – function values, bottom – first derivatives)

time derivative fits well to the values of Series 2. Let

- input Series 1 be given as the observed function values y'_j at instants x_j with weights p_j , $j = 1, 2, \dots, n$;
- input Series 2 as the observed values of first derivatives \bar{y}'_k at instants \bar{x}_k with weights \bar{p}_k , $k = 1, 2, \dots, \bar{n}$;
- output series of the searched function values on the smoothed curve be y_i at the instants x_i containing all values of x_j and \bar{x}_k , $i = 1, 2, \dots, N$, where $N \leq n + \bar{n}$.

In further considerations we shall assume that both input series are defined at all N points x_i , and that the respective weights at the points with no observations are equal to zero.

We define three quantities:

1. Smoothness of the curve (identical with the definition of the original smoothing):

$$S = \frac{1}{x_N - x_1} \int_{x_1}^{x_N} \varphi'''^2(x) dx.$$

Analytical expression of the function $\varphi(x)$ is unknown so the value of its third derivative $\varphi'''(x)$ must be estimated numerically from the smoothed data y . The smoothed curve in the interval between two points $[x_{i+1}; y_{i+1}]$ and $[x_{i+2}; y_{i+2}]$ is defined as a third-order Lagrange polynomial $L_i(x)$ running through the four adjacent points $i, i+1, i+2, i+3$, i.e.

$$L_i(x) = \sum_{k=0}^3 \left(\prod_{\substack{j=0 \\ (j \neq k)}}^3 \frac{(x - x_{i+j})}{(x_{i+k} - x_{i+j})} \right) y_{i+k}.$$

Its third derivative is then equal to

$$L_i'''(x) = \sum_{k=0}^3 \left(6 \prod_{\substack{j=0 \\ (j \neq k)}}^3 \frac{1}{(x_{i+k} - x_{i+j})} \right) y_{i+k}.$$

The third derivatives between each pair of points are given as constants, thus the integral is replaced by a summation:

$$S = \frac{1}{x_N - x_1} \sum_{i=1}^{N-3} \int_{x_{i+1}}^{x_{i+2}} L_i'''(x) dx \quad (1)$$

$$= \sum_{i=1}^{N-3} (a_i y_i + b_i y_{i+1} + c_i y_{i+2} + d_i y_{i+3})^2$$

where

$$a_i = \frac{6\sqrt{(x_{i+2} - x_{i+1})/(x_N - x_1)}}{(x_i - x_{i+1})(x_i - x_{i+2})(x_i - x_{i+3})},$$

$$b_i = \frac{6\sqrt{(x_{i+2} - x_{i+1})/(x_N - x_1)}}{(x_{i+1} - x_i)(x_{i+1} - x_{i+2})(x_{i+1} - x_{i+3})},$$

$$c_i = \frac{6\sqrt{(x_{i+2} - x_{i+1})/(x_N - x_1)}}{(x_{i+2} - x_i)(x_{i+2} - x_{i+1})(x_{i+2} - x_{i+3})},$$

$$d_i = \frac{6\sqrt{(x_{i+2} - x_{i+1})/(x_N - x_1)}}{(x_{i+3} - x_i)(x_{i+3} - x_{i+1})(x_{i+3} - x_{i+2})}.$$

This definition of the smoothness implies that the ideally smooth function (i.e., the one for which $S = 0$) is a quadratic function (and, consequently, its first derivative a linear function) of time. Therefore, the combined estimator proposed in the present paper is different from the original smoothing applied directly to the observed derivatives alone;

2. Fidelity of the smoothed curve to the observed values (almost identical with the definition of the original smoothing):

$$F = \frac{1}{n} \sum_{i=1}^N p_i (y_i' - y_i)^2; \quad (2)$$

3. Fidelity of the smoothed curve to the observed first derivatives (new):

$$\bar{F} = \frac{1}{\bar{n}} \sum_{i=1}^N \bar{p}_i (\bar{y}_i' - \bar{y}_i)^2, \quad (3)$$

in which the smoothed values of first derivatives \bar{y}_i can be expressed in terms of the smoothed function values y_i .

Using the first derivatives of the same Lagrange polynomials $L_i(x)$ that are used to define S we can express $L_i'(x)$, for x lying anywhere in the interval limited by the four adjacent points $i, i+1, i+2, i+3$, as

$$L_i'(x) = A_i(x)y_i + B_i(x)y_{i+1} + C_i(x)y_{i+2} + D_i(x)y_{i+3},$$

in which

$$A_i(x) = \frac{\sum_{\substack{l=0 \\ (l \neq 0)}}^2 \sum_{\substack{m=l+1 \\ (m \neq 0)}}^3 (x - x_{i+l})(x - x_{i+m})}{(x_i - x_{i+1})(x_i - x_{i+2})(x_i - x_{i+3})},$$

$$B_i(x) = \frac{\sum_{\substack{l=0 \\ (l \neq 1)}}^2 \sum_{\substack{m=l+1 \\ (m \neq 1)}}^3 (x - x_{i+l})(x - x_{i+m})}{(x_{i+1} - x_i)(x_{i+1} - x_{i+2})(x_{i+1} - x_{i+3})},$$

$$C_i(x) = \frac{\sum_{\substack{l=0 \\ (l \neq 2)}}^2 \sum_{\substack{m=l+1 \\ (m \neq 2)}}^3 (x - x_{i+l})(x - x_{i+m})}{(x_{i+2} - x_i)(x_{i+2} - x_{i+1})(x_{i+2} - x_{i+3})},$$

$$D_i(x) = \frac{\sum_{\substack{l=0 \\ (l \neq 3)}}^2 \sum_{\substack{m=l+1 \\ (m \neq 3)}}^3 (x - x_{i+l})(x - x_{i+m})}{(x_{i+3} - x_i)(x_{i+3} - x_{i+1})(x_{i+3} - x_{i+2})}.$$

To express the smoothed values of first derivatives \bar{y}_i in Eq. (3) in terms of the smoothed function values y_i , we have a certain freedom of choice of the four points surrounding each of the epochs x_i . We adopt, for the sake of time symmetry, the approach leading to exactly the same solution if the time axis is reversed; the following equations formulate the constraints assuring that the values \bar{y}_i lie on the curve that is the time derivative of the one represented by y_i :

1. For calculating \bar{y}_1 , we use the epochs x_1, x_2, x_3, x_4 ; it means that we have

$$\begin{aligned} \bar{a}_1 &= A_1(x_1), \quad \bar{b}_1 = B_1(x_1), \\ \bar{c}_1 &= C_1(x_1), \quad \bar{d}_1 = D_1(x_1), \\ \bar{y}_1 &= \bar{a}_1 y_1 + \bar{b}_1 y_2 + \bar{c}_1 y_3 + \bar{d}_1 y_4; \end{aligned} \quad (4)$$

2. For calculating \bar{y}_i in the first half of the series, i.e. for $i = 2, 3, \dots, N/2$, we use the epochs $x_{i-1}, x_i, x_{i+1}, x_{i+2}$; it means that we have

$$\begin{aligned} \bar{a}_i &= A_{i-1}(x_i), \quad \bar{b}_i = B_{i-1}(x_i), \\ \bar{c}_i &= C_{i-1}(x_i), \quad \bar{d}_i = D_{i-1}(x_i), \\ \bar{y}_i &= \bar{a}_i y_{i-1} + \bar{b}_i y_i + \bar{c}_i y_{i+1} + \bar{d}_i y_{i+2}; \end{aligned} \quad (5)$$

3. For calculating \bar{y}_i in the second half of the series, i.e. for $i = N/2 + 1, N/2 + 2, \dots, N - 1$, we use the epochs $x_{i-2}, x_{i-1}, x_i, x_{i+1}$; it means that we have

$$\begin{aligned} \bar{a}_i &= A_{i-2}(x_i), \quad \bar{b}_i = B_{i-2}(x_i), \\ \bar{c}_i &= C_{i-2}(x_i), \quad \bar{d}_i = D_{i-2}(x_i), \\ \bar{y}_i &= \bar{a}_i y_{i-2} + \bar{b}_i y_{i-1} + \bar{c}_i y_i + \bar{d}_i y_{i+1}; \end{aligned} \quad (6)$$

4. For calculating \bar{y}_N , we use the epochs $x_{N-3}, x_{N-2}, x_{N-1}, x_N$; it means that we have

$$\begin{aligned} \bar{a}_N &= A_{N-3}(x_N), \quad \bar{b}_N = B_{N-3}(x_N), \\ \bar{c}_N &= C_{N-3}(x_N), \quad \bar{d}_N = D_{N-3}(x_N), \\ \bar{y}_N &= \bar{a}_N y_{N-3} + \bar{b}_N y_{N-2} + \bar{c}_N y_{N-1} + \bar{d}_N y_N. \end{aligned} \quad (7)$$

The expression (3) then can be rewritten as

$$\begin{aligned} \bar{F} &= \frac{1}{\bar{n}} \left[\bar{p}_1 (\bar{y}_1' - \bar{a}_1 y_1 - \bar{b}_1 y_2 - \bar{c}_1 y_3 - \bar{d}_1 y_4)^2 \right. \\ &\quad \left. + \sum_{i=2}^{N/2} \bar{p}_i (\bar{y}_i' - \bar{a}_i y_{i-1} - \bar{b}_i y_i - \bar{c}_i y_{i+1} - \bar{d}_i y_{i+2})^2 \right] \end{aligned} \quad (8)$$

$$+ \sum_{i=N/2+1}^{N-1} \bar{p}_i (\bar{y}'_i - \bar{a}_i y_{i-2} - \bar{b}_i y_{i-1} - \bar{c}_i y_i - \bar{d}_i y_{i+1})^2 + \bar{p}_N (\bar{y}'_N - \bar{a}_N y_{N-3} - \bar{b}_N y_{N-2} - \bar{c}_N y_{N-1} - \bar{d}_N y_N)^2 \Big].$$

We are looking for the smoothed values y_i (and the first derivatives \bar{y}_i corresponding to them) as a compromise among three different conditions, each one applied separately leading to a different solution:

1. The curve should be smooth (i.e., minimizing S);
2. The smoothed values should be close to the observed values of the function (i.e., minimizing F);
3. The first derivatives of the smoothed curve should be close to the observed values of first derivatives (i.e., minimizing \bar{F}).

The adjustment is then done by minimizing a combination of the constraints above, i.e. the expression

$$Q = S + \varepsilon F + \bar{\varepsilon} \bar{F} = \min \quad (9)$$

$$\Rightarrow \frac{\partial Q}{\partial y_i} = 0 \quad \text{for } i = 1, 2, \dots, N,$$

in which $\varepsilon \geq 0$, $\bar{\varepsilon} \geq 0$, obviously leading to the system of N linear equations with unknowns y_i . The degree of compromise among the three conditions is achieved by choosing the values of two parameters: the coefficients of smoothing ε and $\bar{\varepsilon}$ that have respectively the dimensions [time⁻⁶] and [time⁻⁴]. The larger are the values, the larger weight we assign to the fidelity to the observed function values or their first derivatives, and the closer the “smoothed” values are to the observations. To form these equations, we need to express the partial derivatives of S , F and \bar{F} with respect to y_i , in terms of the unknowns y_i and \bar{y}_i .

The partial derivative of S with respect to y_i can be simply expressed as

$$\frac{\partial S}{\partial y_i} = 2(a_i \Delta_i + b_{i-1} \Delta_{i-1} + c_{i-2} \Delta_{i-2} + d_{i-3} \Delta_{i-3}),$$

in which

$$\Delta_i = a_i y_i + b_i y_{i+1} + c_i y_{i+2} + d_i y_{i+3}$$

and

$$a_i = b_i = c_i = d_i = 0 \quad \text{for } i \leq 0 \text{ or } i \geq N - 2.$$

The partial derivative of function F is even simpler:

$$\frac{\partial F}{\partial y_i} = \frac{2p_i(y_i - y'_i)}{n}.$$

More complicated is to express the partial derivatives of \bar{F} ; they are different for different i , due to different choice of \bar{F} in Eq. (8). For sake of shortness, we are using \bar{y}_i in the subsequent equations instead of y_i ; their relations are defined by Eqs. (4–7) above. The first four partial derivatives are

$$\frac{\partial \bar{F}}{\partial y_1} = \frac{2}{n} [\bar{p}_1 \bar{a}_1 (\bar{y}_1 - \bar{y}'_1) + \bar{p}_2 \bar{a}_2 (\bar{y}_2 - \bar{y}'_2)],$$

$$\frac{\partial \bar{F}}{\partial y_2} = \frac{2}{n} [\bar{p}_1 \bar{b}_1 (\bar{y}_1 - \bar{y}'_1) + \bar{p}_2 \bar{b}_2 (\bar{y}_2 - \bar{y}'_2) + \bar{p}_3 \bar{a}_3 (\bar{y}_3 - \bar{y}'_3)],$$

$$\frac{\partial \bar{F}}{\partial y_3} = \frac{2}{n} [\bar{p}_1 \bar{c}_1 (\bar{y}_1 - \bar{y}'_1) + \bar{p}_2 \bar{c}_2 (\bar{y}_2 - \bar{y}'_2) + \bar{p}_3 \bar{b}_3 (\bar{y}_3 - \bar{y}'_3) + \bar{p}_4 \bar{a}_4 (\bar{y}_4 - \bar{y}'_4)],$$

$$\frac{\partial \bar{F}}{\partial y_4} = \frac{2}{n} [\bar{p}_1 \bar{d}_1 (\bar{y}_1 - \bar{y}'_1) + \bar{p}_2 \bar{d}_2 (\bar{y}_2 - \bar{y}'_2) + \bar{p}_3 \bar{c}_3 (\bar{y}_3 - \bar{y}'_3) + \bar{p}_4 \bar{b}_4 (\bar{y}_4 - \bar{y}'_4) + \bar{p}_5 \bar{a}_5 (\bar{y}_5 - \bar{y}'_5)].$$

Then follows a group in the first half of the series, for $i = 5, 6, \dots, N/2 - 2$

$$\frac{\partial \bar{F}}{\partial y_i} = \frac{2}{n} [\bar{p}_{i-2} \bar{d}_{i-2} (\bar{y}_{i-2} - \bar{y}'_{i-2}) + \bar{p}_{i-1} \bar{c}_{i-1} (\bar{y}_{i-1} - \bar{y}'_{i-1}) + \bar{p}_i \bar{b}_i (\bar{y}_i - \bar{y}'_i) + \bar{p}_{i+1} \bar{a}_{i+1} (\bar{y}_{i+1} - \bar{y}'_{i+1})],$$

followed by four derivatives around the center of the series

$$\frac{\partial \bar{F}}{\partial y_{N/2-1}} = \frac{2}{n} [\bar{p}_{N/2-3} \bar{d}_{N/2-3} (\bar{y}_{N/2-3} - \bar{y}'_{N/2-3}) + \bar{p}_{N/2-2} \bar{c}_{N/2-2} (\bar{y}_{N/2-2} - \bar{y}'_{N/2-2}) + \bar{p}_{N/2-1} \bar{b}_{N/2-1} (\bar{y}_{N/2-1} - \bar{y}'_{N/2-1}) + \bar{p}_{N/2} \bar{a}_{N/2} (\bar{y}_{N/2} - \bar{y}'_{N/2}) + \bar{p}_{N/2+1} \bar{a}_{N/2+1} (\bar{y}_{N/2+1} - \bar{y}'_{N/2+1})],$$

$$\frac{\partial \bar{F}}{\partial y_{N/2}} = \frac{2}{n} [\bar{p}_{N/2-2} \bar{d}_{N/2-2} (\bar{y}_{N/2-2} - \bar{y}'_{N/2-2}) + \bar{p}_{N/2-1} \bar{c}_{N/2-1} (\bar{y}_{N/2-1} - \bar{y}'_{N/2-1}) + \bar{p}_{N/2} \bar{b}_{N/2} (\bar{y}_{N/2} - \bar{y}'_{N/2}) + \bar{p}_{N/2+1} \bar{b}_{N/2+1} (\bar{y}_{N/2+1} - \bar{y}'_{N/2+1}) + \bar{p}_{N/2+2} \bar{a}_{N/2+2} (\bar{y}_{N/2+2} - \bar{y}'_{N/2+2})],$$

$$\frac{\partial \bar{F}}{\partial y_{N/2+1}} = \frac{2}{n} [\bar{p}_{N/2-1} \bar{d}_{N/2-1} (\bar{y}_{N/2-1} - \bar{y}'_{N/2-1}) + \bar{p}_{N/2} \bar{c}_{N/2} (\bar{y}_{N/2} - \bar{y}'_{N/2}) + \bar{p}_{N/2+1} \bar{c}_{N/2+1} (\bar{y}_{N/2+1} - \bar{y}'_{N/2+1}) + \bar{p}_{N/2+2} \bar{b}_{N/2+2} (\bar{y}_{N/2+2} - \bar{y}'_{N/2+2}) + \bar{p}_{N/2+3} \bar{a}_{N/2+3} (\bar{y}_{N/2+3} - \bar{y}'_{N/2+3})],$$

$$\frac{\partial \bar{F}}{\partial y_{N/2+2}} = \frac{2}{n} [\bar{p}_{N/2} \bar{d}_{N/2} (\bar{y}_{N/2} - \bar{y}'_{N/2}) + \bar{p}_{N/2+1} \bar{d}_{N/2+1} (\bar{y}_{N/2+1} - \bar{y}'_{N/2+1}) + \bar{p}_{N/2+2} \bar{c}_{N/2+2} (\bar{y}_{N/2+2} - \bar{y}'_{N/2+2}) + \bar{p}_{N/2+3} \bar{b}_{N/2+3} (\bar{y}_{N/2+3} - \bar{y}'_{N/2+3}) + \bar{p}_{N/2+4} \bar{a}_{N/2+4} (\bar{y}_{N/2+4} - \bar{y}'_{N/2+4})].$$

In the second half of the series, i.e. for $i = N/2+3, N/2+4, \dots, N-4$, we have

$$\frac{\partial \bar{F}}{\partial y_i} = \frac{2}{n} [\bar{p}_{i-1} \bar{d}_{i-1} (\bar{y}_{i-1} - \bar{y}'_{i-1}) + \bar{p}_i \bar{c}_i (\bar{y}_i - \bar{y}'_i) + \bar{p}_{i+1} \bar{b}_{i+1} (\bar{y}_{i+1} - \bar{y}'_{i+1}) + \bar{p}_{i+2} \bar{a}_{i+2} (\bar{y}_{i+2} - \bar{y}'_{i+2})],$$

and the last four partial derivatives read

$$\begin{aligned}\frac{\partial \bar{F}}{\partial y_{N-3}} &= \frac{2}{\bar{n}} [\bar{p}_{N-4} \bar{d}_{N-4} (\bar{y}_{N-4} - \bar{y}'_{N-4}) \\ &\quad + \bar{p}_{N-3} \bar{c}_{N-3} (\bar{y}_{N-3} - \bar{y}'_{N-3}) \\ &\quad + \bar{p}_{N-2} \bar{b}_{N-2} (\bar{y}_{N-2} - \bar{y}'_{N-2}) \\ &\quad + \bar{p}_{N-1} \bar{a}_{N-1} (\bar{y}_{N-1} - \bar{y}'_{N-1}) + \bar{p}_N \bar{a}_N (\bar{y}_N - \bar{y}'_N)], \\ \frac{\partial \bar{F}}{\partial y_{N-2}} &= \frac{2}{\bar{n}} [\bar{p}_{N-3} \bar{d}_{N-3} (\bar{y}_{N-3} - \bar{y}'_{N-3}) \\ &\quad + \bar{p}_{N-2} \bar{c}_{N-2} (\bar{y}_{N-2} - \bar{y}'_{N-2}) \\ &\quad + \bar{p}_{N-1} \bar{b}_{N-1} (\bar{y}_{N-1} - \bar{y}'_{N-1}) + \bar{p}_N \bar{b}_N (\bar{y}_N - \bar{y}'_N)], \\ \frac{\partial \bar{F}}{\partial y_{N-1}} &= \frac{2}{\bar{n}} [\bar{d}_{N-2} \bar{c}_{N-2} (\bar{y}_{N-2} - \bar{y}'_{N-2}) \\ &\quad + \bar{p}_{N-1} \bar{c}_{N-1} (\bar{y}_{N-1} - \bar{y}'_{N-1}) + \bar{p}_N \bar{c}_N (\bar{y}_N - \bar{y}'_N)], \\ \frac{\partial \bar{F}}{\partial y_N} &= \frac{2}{\bar{n}} [\bar{p}_{N-1} \bar{d}_{N-1} (\bar{y}_{N-1} - \bar{y}'_{N-1}) \\ &\quad + \bar{p}_N \bar{d}_N (\bar{y}_N - \bar{y}'_N)].\end{aligned}$$

2.2. Algorithm to compose the equations

From the preceding subsection it follows that the matrix of the system of linear Eqs. (9) is sparse, with only seven diagonals centered around main diagonal containing non-zero elements. The matrix is symmetric and singular for $\varepsilon = 0$ (the sum of elements in the i -th row is equal to $\varepsilon p_i/n$). To calculate the elements we use the algorithm described below.

1. We successively put into each i -th element on the main diagonal of the matrix the values $\varepsilon p_i/n$, and we put into the right-hand-sides of the equations the values $\varepsilon p_i y'_i/n$ (this part corresponds to constraint F);
2. For $i = 1, 2, \dots, N-3$ we add successively to each i -th 4×4 submatrix centered around main diagonal the matrix

$$\begin{pmatrix} a_i^2 & a_i b_i & a_i c_i & a_i d_i \\ b_i a_i & b_i^2 & b_i c_i & b_i d_i \\ c_i a_i & c_i b_i & c_i^2 & c_i d_i \\ d_i a_i & d_i b_i & d_i c_i & d_i^2 \end{pmatrix}$$

(this part corresponds to constraint S).

3. For $i = 1, 2, \dots, N$ we successively calculate the matrix

$$\frac{\varepsilon \bar{p}_i}{\bar{n}} \begin{pmatrix} \bar{a}_i^2 & \bar{a}_i \bar{b}_i & \bar{a}_i \bar{c}_i & \bar{a}_i \bar{d}_i \\ \bar{b}_i \bar{a}_i & \bar{b}_i^2 & \bar{b}_i \bar{c}_i & \bar{b}_i \bar{d}_i \\ \bar{c}_i \bar{a}_i & \bar{c}_i \bar{b}_i & \bar{c}_i^2 & \bar{c}_i \bar{d}_i \\ \bar{d}_i \bar{a}_i & \bar{d}_i \bar{b}_i & \bar{d}_i \bar{c}_i & \bar{d}_i^2 \end{pmatrix}$$

and the column vector

$$\frac{\varepsilon \bar{p}_i}{\bar{n}} \begin{pmatrix} \bar{a}_i \bar{y}'_i \\ \bar{b}_i \bar{y}'_i \\ \bar{c}_i \bar{y}'_i \\ \bar{d}_i \bar{y}'_i \end{pmatrix}$$

from $\bar{a}_i, \bar{b}_i, \bar{c}_i, \bar{d}_i$ given by one of the Eqs. (4), (5), (6) or (7), depending on i .

If $i = 1$, we add them respectively to the first 4×4 submatrix centered around the main diagonal (i.e., to the one with indices 1, 2, 3 and 4) and to the four corresponding right-hand-sides.

If $i = 2, 3, \dots, N/2$, we add them respectively to the 4×4 submatrices centered around the main diagonal with indices $i-1, i, i+1$ and $i+2$ and to the four corresponding right-hand-sides.

If $i = N/2 + 1, N/2 + 2, \dots, N-1$, we add them respectively to the 4×4 submatrices centered around the main diagonal with indices $i-2, i-1, i$ and $i+1$ and to the four corresponding right-hand-sides.

Finally, if $i = N$, we add them to the last 4×4 submatrix centered around the main diagonal (i.e., to the one with indices $N-3, N-2, N-1$ and N) and to the four corresponding right-hand-sides.

(this part corresponds to constraint \bar{F}).

If we wish to normalize the weights in both input series (i.e., if we require that the average weights in Series 1 and Series 2 are identically equal to unity), we simply replace n, \bar{n} in the expressions above by $\sum_1^N p_i, \sum_1^N \bar{p}_i$, respectively. The software that we use in all subsequent tests and examples follows namely this approach.

2.3. Numerical solution

By solving the system of linear equations formed above we arrive at the smoothed function values y_i , referred to the instants x_i ; to obtain the smoothed first derivative values \bar{y}_i , the constraints (4), (5), (6) or (7) are then used.

To solve the system, we can use a standard Gaussian elimination method, as proposed in original smoothing (Vondrák 1969). This is a very simple and straightforward procedure in which we can easily make use of the important properties of the matrix; it is symmetric and sparse.

However, as we shall prove, the system is positive definite and we know that the symmetric factorization exists and moreover is stable to compute. Apart from the unknowns we sometimes need to estimate the uncertainties of the smoothed values or their functions. Therefore we follow a similar procedure as proposed by us for the case of observed values without first derivatives (Čepek & Vondrák 2000) enabling to calculate easily not only the unknowns but also their covariances.

In matrix notation we can rewrite the system of Eqs. (9) simply as

$$\mathbf{A} \mathbf{y} = \mathbf{B} \begin{pmatrix} \mathbf{y}' \\ \bar{\mathbf{y}}' \end{pmatrix}, \quad \mathbf{B} = (\mathbf{B}_1 \mathbf{B}_2), \quad (10)$$

where submatrices $\mathbf{B}_1, \mathbf{B}_2$ have the form

$$\mathbf{B}_1 = \frac{\varepsilon}{n} \text{diag}\{p_1, \dots, p_n\}$$

and

$$\mathbf{B}_2 = \frac{\bar{\varepsilon}}{n} \begin{pmatrix} \bar{p}_1 \bar{a}_1 & 0 \\ \bar{p}_1 \bar{b}_1 & \\ \bar{p}_1 \bar{c}_1 & \\ \bar{p}_1 \bar{d}_1 & \cdots & \bar{p}_n \bar{a}_n \\ & & \bar{p}_n \bar{b}_n \\ & & \bar{p}_n \bar{c}_n \\ 0 & & \bar{p}_n \bar{d}_n \end{pmatrix}.$$

Matrix \mathbf{A} is a symmetric band matrix. The bandwidth of \mathbf{A} is equal to only three

$$\beta(\mathbf{A}) = \max\{|i - j| \mid a_{ij} \neq 0\} = 3.$$

We store only the symmetric part of the matrix \mathbf{A} in N by 3+1 vectors.

Following the algorithm to compose the equations given in the Sect. 2.2 we can express the matrix as the summation

$$\mathbf{A} = \begin{pmatrix} \varepsilon p_1/n & & 0 \\ & \ddots & \\ 0 & & \varepsilon p_N/n \end{pmatrix} + \sum_{i=1}^{2N-3} \begin{pmatrix} \ddots & & 0 \\ & \mathbf{D}_i & \\ 0 & & \ddots \end{pmatrix},$$

where the structure of coefficients in all diagonal blocks is

$$\mathbf{D}_i = \begin{pmatrix} aa & ab & ac & ad \\ ba & bb & bc & bd \\ ca & cb & cc & cd \\ da & db & dc & dd \end{pmatrix} = \begin{pmatrix} a \\ b \\ c \\ d \end{pmatrix} (a \ b \ c \ d).$$

All diagonal elements $\varepsilon p_i/n$ are nonnegative and all diagonal blocks \mathbf{D}_i are clearly positive semidefinite. Resulting matrix \mathbf{A} is thus positive semidefinite as well.

Supposing that the matrix \mathbf{A} is regular, it follows that the semidefinite symmetric matrix \mathbf{A} is positive definite and we can use Cholesky factorization to solve the system (10).

We use the variant of Cholesky factorization

$$\mathbf{A} = \mathbf{U}^T \mathbf{D} \mathbf{U}$$

where \mathbf{D} is diagonal matrix and \mathbf{U} is upper triangular matrix with unit diagonal. The bandwidth $\beta(\mathbf{U}) = 3$ is the same as the bandwidth of \mathbf{A} . With the unique Cholesky factorization of matrix \mathbf{A} the solution of system of Eqs. (10) is obtained simply by solving two band triangular systems (forward and backward substitution)

$$\mathbf{U}^T \mathbf{w} = \mathbf{B} \mathbf{y}', \quad \mathbf{U} \mathbf{x} = \mathbf{D}^{-1} \mathbf{w}.$$

We can estimate the standard deviation of smoothed values from (2) as

$$\sigma_0 = \sqrt{\frac{\sum_{i=1}^N p_i (y_i - y'_i)^2}{n}} = \sqrt{F}.$$

Smoothed values are linear combinations of observed values

$$\mathbf{y} = \mathbf{A}^{-1} \mathbf{z} = \mathbf{A}^{-1} \mathbf{B} \begin{pmatrix} \mathbf{y}' \\ \bar{\mathbf{y}}' \end{pmatrix}.$$

Its covariance matrix Σ_{yy} is, according to the general principle of propagation of variances and covariances of linear functions

$$\Sigma_{yy} = \mathbf{A}^{-1} \Sigma_{zz} \mathbf{A}^{-1} = \mathbf{A}^{-1} \mathbf{B} \begin{pmatrix} \Sigma_{y'y'} & 0 \\ 0 & \Sigma_{\bar{y}'\bar{y}'} \end{pmatrix} \mathbf{B}^T \mathbf{A}^{-1}. \quad (11)$$

In the special case of smoothing observations without measured time derivatives, vector $\bar{\mathbf{y}}'$ and submatrix \mathbf{B}_2 are missing in the Eq. (10), inverse of Σ_{yy} is a band matrix and we can compute only selected subset band of Σ_{yy} as described in (Čepek & Vondrák 2000). With measured first derivatives we have to invert the full matrix \mathbf{A} to express covariances of smoothed values \mathbf{y} , but inverting symmetric positive matrix is an easy task and we can exploit the fact that variance-covariance matrix Σ_{zz} is a band matrix with bandwidth three.

2.4. Some properties of the filter, choice of coefficients of smoothing

As already stated above, the matrix of the system is singular for $\varepsilon = 0$ (this is equivalent to a case when we have observations of first derivatives only); in such a case, there exists no unique solution of the problem unless we impose an additional constraint. This can be done, e.g., by requiring that the smoothed curve runs through one point, either observed or arbitrarily chosen. In this case, we can simply put 1 into the main diagonal of any row of the matrix (see step 1 of Sect. 2.2) and the chosen function value to the corresponding right-hand-side. From this also follows that we always need at least one observation of function value with non-zero weight (the observations of first derivatives alone are not sufficient).

On the other hand, there arises no problem at all if $\bar{\varepsilon} = 0$ and $\varepsilon \neq 0$ (equivalent to a case with no observations of first derivatives); in this case, the problem reduces to original smoothing, and the observed first derivatives are simply ignored.

A really serious problem arises only if both $\varepsilon = 0$ and $\bar{\varepsilon} = 0$. Then we have a singular matrix with the deficiency equal to three, and any quadratic parabola satisfies the system of Eqs. (9). Then we have a freedom of choosing three additional constraints (not linearly dependent); e.g., we can choose any three values (at different epochs) on the curve, we can do a quadratic regression to the observed function values, a combined regression to fit the parabola both to observed function and first derivative values, etc.

There is a close relation between the coefficients of smoothing and the transfer function T of the filter (i.e., the ratio between the amplitude of the smoothed curve and the observed amplitude of a periodic function with frequency f). The transfer function for the function values (identical with the original smoothing) was analytically expressed by Huang & Zhou (1981, 1982), assuming the weights p_i equal to unity, as

$$T = \frac{1}{1 + \varepsilon^{-1} (2\pi f)^6}. \quad (12)$$

Similarly, we can express the transfer function \bar{T} for the observed first derivatives in terms of $\bar{\varepsilon}$ and frequency f :

$$\bar{T} = \frac{1}{1 + \bar{\varepsilon}^{-1} (2\pi f)^4}. \quad (13)$$

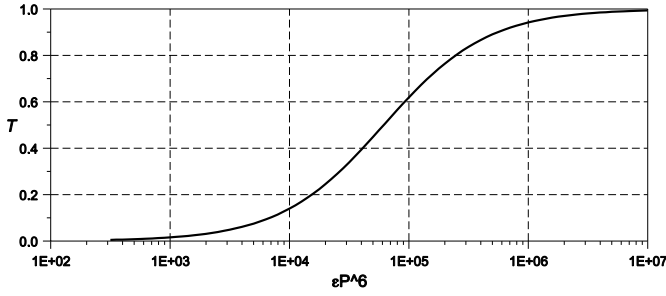


Fig. 2. Transfer function T for the measured function values, plotted as function of εP^6

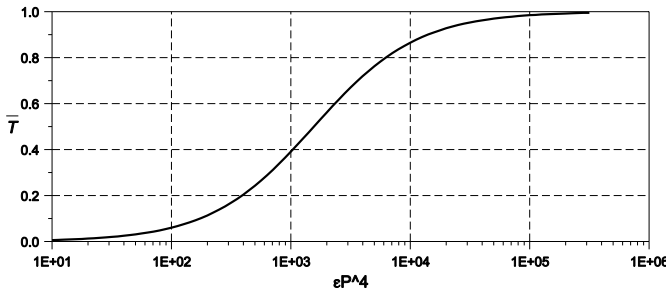


Fig. 3. Transfer function \bar{T} for the measured first derivatives, plotted as function of $\bar{\varepsilon} P^4$

Both transfer functions are graphically displayed in Figs. 2 and 3, where they are plotted against dimensionless arguments εP^6 and $\bar{\varepsilon} P^4$ ($P = 1/f$ is the period) in logarithmic scale.

It is necessary to say that these transfer functions are strictly valid only in cases when either only function values, or only first derivatives (plus one arbitrarily chosen function value, as mentioned above) are observed. When both types of observations are mixed in one solution, a transfer function lying somewhere between the two is reflected in the smoothed series, depending on the ratio of the numbers of both types of observation.

In principle, there are two possibilities of choosing the coefficients of smoothing ε and $\bar{\varepsilon}$, both requiring at least an approximate a priori knowledge of the observed process; we should have a realistic estimation of either the precision of the measurement, or the shortest period contained in the signal:

1. Knowing a priori average values of standard errors in Series 1 and 2, we try to find such coefficients of smoothing that would yield the same estimated a posteriori standard errors from the dispersion of observations around the smoothed curve (these can be easily obtained as $\sqrt{\bar{F}}$, $\sqrt{\bar{F}'}$). This approach requires the solution in several steps, by iterations. It often appears that the satisfactory solution is impossible to find, especially if the a priori standard errors are unrealistically small and both series of observed values and first derivatives are not mutually compatible on this level of accuracy (see next sections for tests with

simulated data, practical examples and more detailed discussion). Then higher values than a priori standard errors must be used, or the following possibility of choosing coefficients of smoothing should be taken;

2. Knowing in advance which frequencies we aim to suppress in both observed series, we use the transfer functions of Eqs. (12), (13) to calculate the corresponding values of ε and $\bar{\varepsilon}$, and use the method as a low pass filter. Here we can apply a very simple rule; denoting the period for which half of the amplitude is suppressed as $P_{0.5}$, i.e. corresponding to $T = \bar{T} = 0.5$ (shorter periods are suppressed more, longer periods less), we calculate both coefficients of smoothing as

$$\varepsilon(P_{0.5}) = \left(\frac{2\pi}{P_{0.5}}\right)^6, \quad \bar{\varepsilon}(P_{0.5}) = \left(\frac{2\pi}{P_{0.5}}\right)^4. \quad (14)$$

Alternatively, slightly different formulas hold for calculating the coefficients of smoothing if we wish to pass 99% of the amplitude of a periodic process with period $P_{0.99}$ (corresponding to $T = \bar{T} = 0.99$):

$$\varepsilon(P_{0.99}) = 99 \left(\frac{2\pi}{P_{0.99}}\right)^6, \quad \bar{\varepsilon}(P_{0.99}) = 99 \left(\frac{2\pi}{P_{0.99}}\right)^4.$$

This approach is especially suitable in cases when we require more heavily smoothed series (with only low frequencies retained) for special analyses, or if we apply the method twice, to retain only the frequencies in a specific frequency range as proposed for original smoothing in (Vondrák 1977).

2.5. Testing the method with simulated data

Before using the method with real observations, it is reasonable to test it with simulated data, with the expected results to be known beforehand. We selected simulated data series that are very similar to what can be encountered in reality. Namely we used the signal resembling UT1 series, consisting of three periodic terms – annual, semi-annual and fortnightly – of the form (in time seconds):

$$y = -0.020 \sin 2\pi t + 0.012 \cos 2\pi t + 0.006 \sin 4\pi t - 0.007 \cos 4\pi t + 0.0008 \sin 52\pi t,$$

in which $t = (x - 50448)/365.2422$ is the argument expressed in years. Its first derivative with respect to time argument x is then

$$\bar{y} = \pi(-0.040 \cos 2\pi t - 0.024 \sin 2\pi t + 0.024 \cos 4\pi t + 0.028 \sin 4\pi t + 0.0416 \cos 52\pi t)/365.2422.$$

We generated the series y , \bar{y} at one-day spacing, covering the interval 400 days long, and added to both of them Gaussian random noise with rms dispersion equal to $10 \mu s$ and $10 \mu s/\text{day}$, respectively. Both series (in which all weights were put equal to 1) were then subject to combined smoothing described above, using numerous pairs of coefficients of smoothing ε , $\bar{\varepsilon}$. The tests led to the

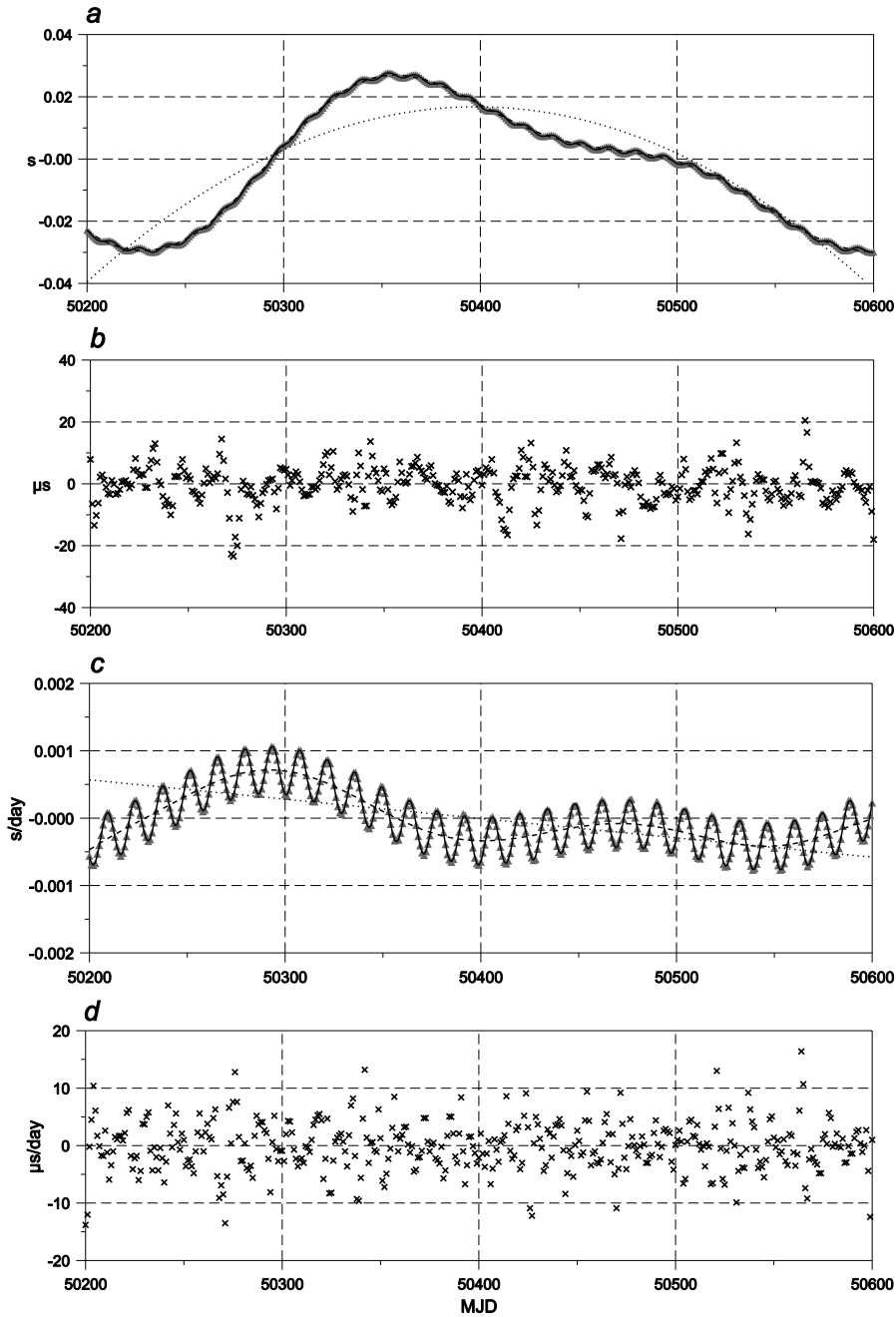


Fig. 4. Combined smoothing of simulated data, consisting of three harmonic oscillations plus random noise. Grey triangles in subplots **a**) (function values y) and **c**) (values of first derivative \dot{y}) represent the input data, full, dashed and dotted lines in the same subplots depict the smoothed curves with stronger and stronger smoothing. Differences between the weakest smoothing (full lines in subplots **a**, **c**) and original signal are displayed as crosses in subplots **b**) and **d**), in highly enlarged scale

following findings:

- In order to get the best approximation of the signal, it is recommendable to choose the values $\varepsilon(P_{0.5})$, $\bar{\varepsilon}(P_{0.5})$ as given by Eqs. (14) for $P_{0.5}$ lying approximately between one third and one half of the shortest known period contained in the signal. Alternatively, it is also possible to calculate $\varepsilon(P_{0.99})$, $\bar{\varepsilon}(P_{0.99})$ from Eqs. (15), in which we put $P_{0.99}$ equal to the shortest known period of the signal. Any values of ε , $\bar{\varepsilon}$ lying in the vicinity of these yield approximately the same acceptable results;
- Substantially larger values of ε , $\bar{\varepsilon}$ than given above lead to more “ragged” curves in which the noise of the observations is less suppressed;
- Using substantially smaller values of ε , $\bar{\varepsilon}$ leads to smoother curves in which the short-periodic part of the signal is suppressed;

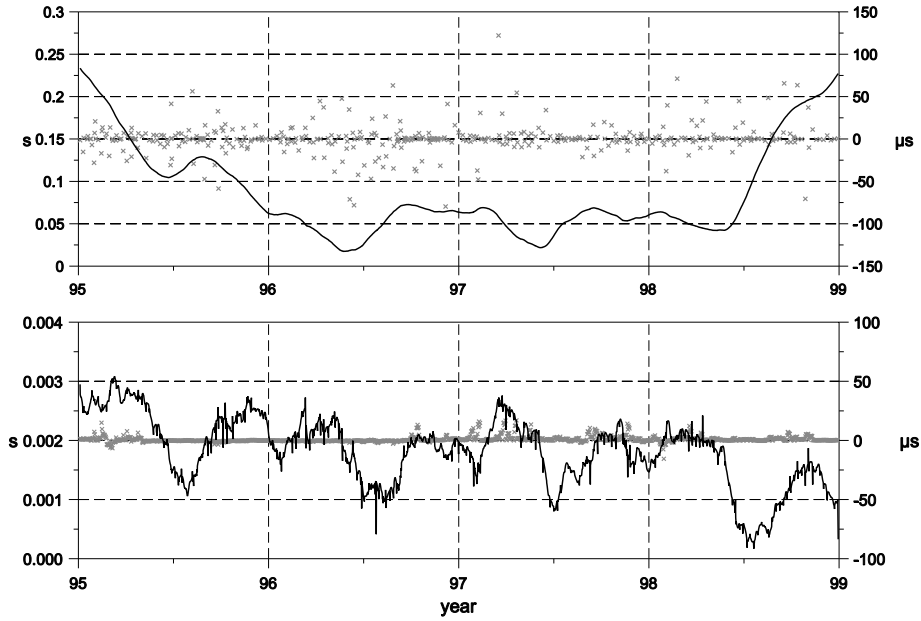


Fig. 5. Combined smoothing of UT1R-TAI measured by VLBI and lodR measured by GPS, using $\varepsilon = 25 \cdot 10^2 \text{ day}^{-6}$, $\bar{\varepsilon} = 4 \cdot 10^4 \text{ day}^{-4}$ (leading to dispersions equal to formal standard errors). Smoothed curves are shown as full lines and residuals (enlarged scale on the right) as grey crosses. Reduced values of $\text{UT1R-TAI} + 27.5 + 0.00183(\text{MJD} - 48987)$ are displayed in top, lodR in bottom

- Using substantially smaller value of $\bar{\varepsilon}$ (with ε kept according to the rule above) does not do much harm; it only applies lower weights to all observed first derivatives (extreme case $\bar{\varepsilon} = 0$ neglects these observations completely). This variant can be used if we are sure that the quality of these observations is not very good;
- Using substantially larger value of $\bar{\varepsilon}$ (keeping ε as calculated above) leads generally to unsatisfactory results, especially if the epochs of both series do not coincide (see the first example with real data in Sect. 3 below).

An illustration of combining the simulated data with different values of ε , $\bar{\varepsilon}$ is given in Fig. 4. The simulated observations of y (plot *a*) and \bar{y} (plot *c*) are depicted as grey triangles. Three different sets of ε , $\bar{\varepsilon}$ are used:

1. $\varepsilon = \bar{\varepsilon} = 0$, leading to a quadratic function of y , and a straight line of \bar{y} , both being calculated as best fit to both data series. These results are displayed as dotted lines;
2. $\varepsilon = 3.5 \cdot 10^{-7} \text{ day}^{-6}$, $\bar{\varepsilon} = 4.9 \cdot 10^{-5} \text{ day}^{-4}$ (corresponding to $P_{0.5} = 75$ days), given as dashed lines. This estimator almost exactly follows the annual and semi-annual term and completely suppresses the fortnightly term;
3. $\varepsilon = 3.9 \text{ day}^{-6}$, $\bar{\varepsilon} = 2.5 \text{ day}^{-4}$ (corresponding to $P_{0.5} = 5$ days), represented by full lines. It almost perfectly reproduces the complete signal. The differences of this smoothed curve from either “observed” values or the signal are so small that they cannot be seen in the given scale. Therefore, the differences between the smoothed curves and the original signal are displayed

in the same graph, highly enlarged (1000 and 100 times in plots *b* and *d*, respectively). The rms difference between the smoothed curves of y and \bar{y} and the original signal is respectively $5.9 \mu\text{s}$ and $4.3 \mu\text{s}/\text{day}$, which are equal approximately to only one half of the noise in the input data.

We also made a number of tests with the same simulated data in which the function values y , sampled only once per 7 days, were combined with \bar{y} values at daily intervals. We also made tests with the epochs of y shifted with respect to \bar{y} by small fractions of the day (0.1d and 0.01d). The results were almost equivalent to the previous ones, and we came to conclusion that the same rules of choosing the coefficients ε , $\bar{\varepsilon}$ as described above can be applied even in these cases.

3. Combination of Earth orientation parameters

The International Earth Rotation Service (IERS), founded in 1988 jointly by the IAU and IUGG, mainly in order to monitor the Earth orientation parameters (Universal Time, polar motion and celestial pole offsets), collects and analyzes the observations by several space techniques. They comprise already mentioned VLBI and GPS, but also satellite laser ranging (SLR), lunar laser ranging (LLR) and, most recently, Doppler orbit determination and radiopositioning integrated on satellite (DORIS). Now the discussions take place within IERS how to combine the results of all these techniques into a single representative solution. The proposed method

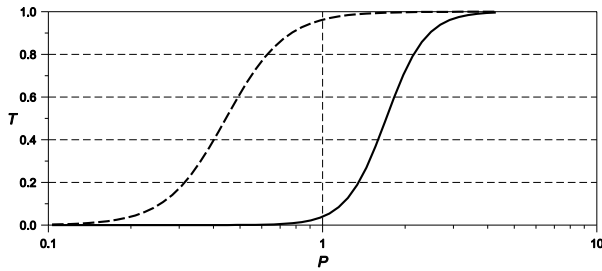


Fig. 6. Transfer functions of the smoothing used to combine the data in Fig. 5, plotted against period P in days (full line corresponds to $\varepsilon = 25 \cdot 10^2 \text{ day}^{-6}$, dashed line to $\bar{\varepsilon} = 4 \cdot 10^4 \text{ day}^{-4}$)

of combined smoothing is a contribution to solving this problem.

The accuracy of these techniques sometimes strongly depend on the frequency of the observed phenomenon, as demonstrated e.g. by Vondrák & Gambis (2000). The most striking difference is between VLBI (that refers the observations to extragalactic objects) and satellite methods (that refer the observations to the orbits of the satellites). The motions of extragalactic objects with respect to inertial reference system are negligible, therefore the stability of the celestial frame is very high at any frequency. On the other hand, the motions of the satellite orbits with respect to inertial reference system depend not only on the gravitational field of the Earth and its time changes but also on numerous non-gravitational forces. Therefore these motions can be modeled with uncertainties that grow with period.

The most important consequence is that only the short-periodic part of Universal Time can be measured by satellite methods what is in practice assured by determining the length-of-day changes instead of Universal Time. On the other hand, the satellite methods are capable of providing much more frequent measurements, monitoring thus shorter periodic motions of the Earth's orientation in space and their time derivatives.

In the following we demonstrate the capability of the method proposed above to combine Universal Time with length-of-day changes, and polar motion with its time derivatives.

3.1. Combining Universal Time and length-of-day changes

As already said in the Introduction, the proposed method is especially convenient to combine the observations of Universal Time, in the form of its difference from the uniform time scale given by atomic clocks (UT1–TAI, observed weekly by VLBI) and the length of day changes (l.o.d., observed daily by GPS). We chose the series covering four years (1995.0–1999.0) as determined at Shanghai Astronomical Observatory, China (VLBI), and at the Astronomical Institute of Berne University, Switzerland

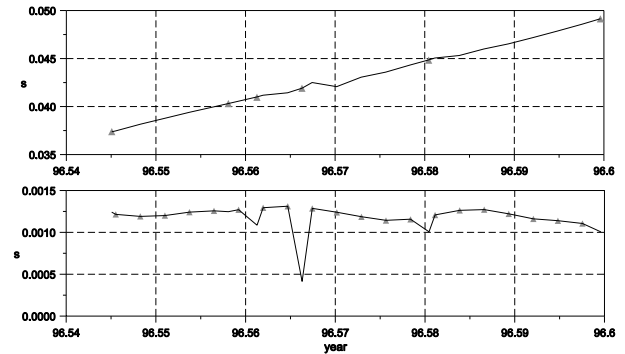


Fig. 7. Enlarged cutoff of Fig. 5 around a spurious peak caused by improper choice of coefficients of smoothing (UT1R in top, lodR in bottom)

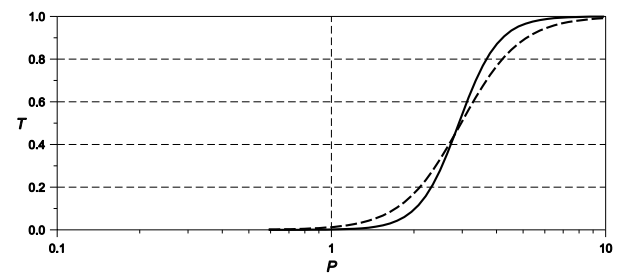


Fig. 8. Transfer functions of the smoothing used to combine the data in Figs. 9, 10 and 11, plotted against period P in days (full line corresponds to $\varepsilon = 100 \text{ day}^{-6}$, dashed line to $\bar{\varepsilon} = 20 \text{ day}^{-4}$)

(GPS). The two observed quantities are tied by a simple relation:

$$\text{l.o.d.} = -d(\text{UT1} - \text{TAI})/dt,$$

in which l.o.d. is given in seconds of time if the time derivative on the r.h.s. is expressed in seconds of time per day. Before using both series in the combination, we removed from them the theoretical solid Earth tidal variations with periods shorter than 35 days after Yoder et al. (1981); these corrections lead to series denoted as UT1R–TAI and lodR. The a priori values of the average standard deviations of both series are $7.3 \mu\text{s}$ for UT1 of VLBI and $1.5 \mu\text{s}$ for l.o.d. of GPS.

Firstly, we applied a set of coefficients of smoothing that makes a posteriori standard deviations equal to their average a priori values, using iterations as outlined in Sect. 2.4 (namely $\varepsilon = 25 \cdot 10^2 \text{ day}^{-6}$, $\bar{\varepsilon} = 4 \cdot 10^4 \text{ day}^{-4}$). The results are shown in Fig. 5, UT1R in top and lodR in bottom part of the figure. The values UT1R–TAI have a very large negative trend; therefore we plot their reduced values, with a constant and linear trend removed. Since the observed values are hardly distinguishable from the smoothed curve (black full line), the residuals in the sense “observed – smoothed” (displayed as gray crosses) are plotted in the enlarged scale marked on the right. The full line in lower graph is negatively taken time derivative of the one in the upper part.

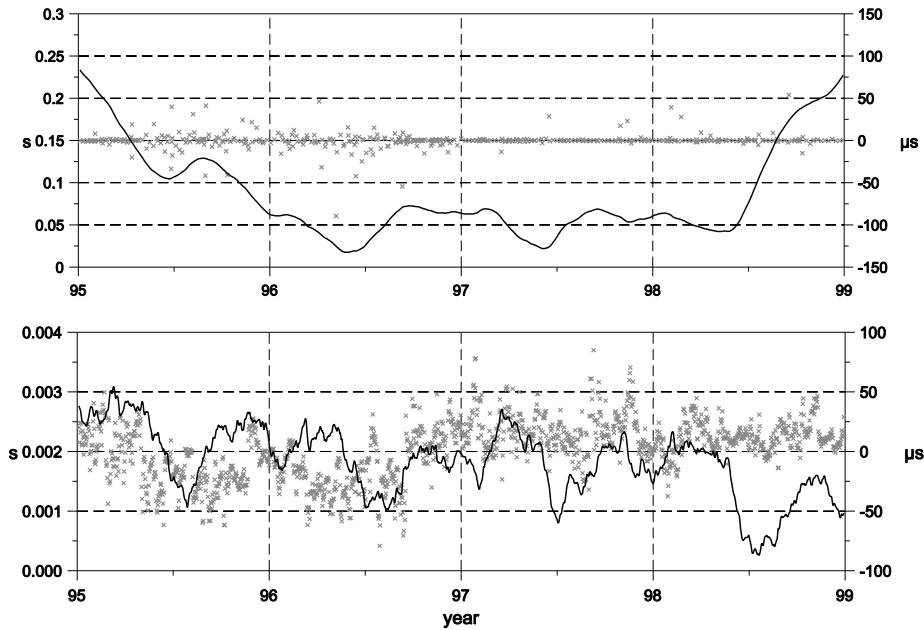


Fig. 9. Combined smoothing of UT1R-TAI measured by VLBI and lodR measured by GPS, using $\varepsilon = 100 \text{ day}^{-6}$, $\bar{\varepsilon} = 20 \text{ day}^{-4}$ (leading to standard deviations equal to $2.6 \mu\text{s}$ and $24.8 \mu\text{s}$, respectively). Smoothed curves are shown as full lines and residuals (enlarged scale on the right) as grey crosses. Reduced values of UT1R-TAI+27.5+0.00183(MJD-48987) are displayed in top, lodR in bottom.

The combined smoothing, applied in this case, has transfer function plotted in Fig. 6. It is a very weak smoothing that passes completely all periods longer than approximately one day, too weak to remove the true noise of the observations as one can see from the lower curve of lodR that is rather ragged.

As the tests with simulated data revealed (see Sect. 2.5 above), the combined smoothing with this combination of ε , $\bar{\varepsilon}$ should not generally give satisfactory results. Really, a detailed inspection of the results discloses that the smoothed curve, although running almost perfectly through both series of observed values, sometimes forms sudden spurious peaks between two points with l.o.d. observations, at the epochs with only UT1 observed. A typical example of this effect is demonstrated in Fig. 7 that is a closeup of a part of Fig. 5. This effect is due to the very weak smoothing applied (almost interpolation in this case), and also because much weaker smoothing (large value of $\bar{\varepsilon}$) is used for observed first derivatives.

Therefore we made another try and used a stronger smoothing, following the rules given in Sect. 2.5. We assumed that the shortest period of the signal contained in the data is about one week; using $P_{0.5} = 3$ days to calculate the coefficients of smoothing (see Sect. 2.4) leads to $\varepsilon = 100 \text{ day}^{-6}$, $\bar{\varepsilon} = 20 \text{ day}^{-4}$. The solution yields a posteriori standard deviations equal to $2.6 \mu\text{s}$ and $24.8 \mu\text{s}$, respectively, the values that are evidently much different from the average a priori values given by the analysis centers.

The result is displayed in Fig. 9, and the transfer functions are given in Fig. 8; they are shifted to the right

with respect to the ones depicted in Fig. 6 and they are nearly identical. This combination gives much better results than the preceding one; the smoothing is still rather weak not to suppress real signal but sufficiently efficient to remove the observational noise. The residuals disclose that UT1 as observed by VLBI seems to be very accurate (maybe more than one would expect from their formal standard deviations). The l.o.d. values as given by GPS are obviously more noisy than their formal standard deviations hint – they rather represent the internal precision of the method (without taking into account the instabilities of the modeled satellite orbits with respect to inertial reference frame) than accuracy. The residuals of lodR thus mostly reflect the long-periodic deviations of GPS-determined lod that are not fully compatible with the first derivative of VLBI-based UT1. The behavior of the residuals e.g. clearly demonstrate that the l.o.d. as determined by GPS before and after 1996.7 systematically differ by about $40 \mu\text{s}$. It is necessary to mention in this respect that Berne University is probably the only GPS analysis center that provides the free solution of l.o.d., without frequent constraints to VLBI results, and that the date of systematic step in the results correspond to the change in the model used by this center.

3.2. Combining polar motion and its rate

Another example of using the new method is given by the observation of polar motion; Astronomical Institute of the

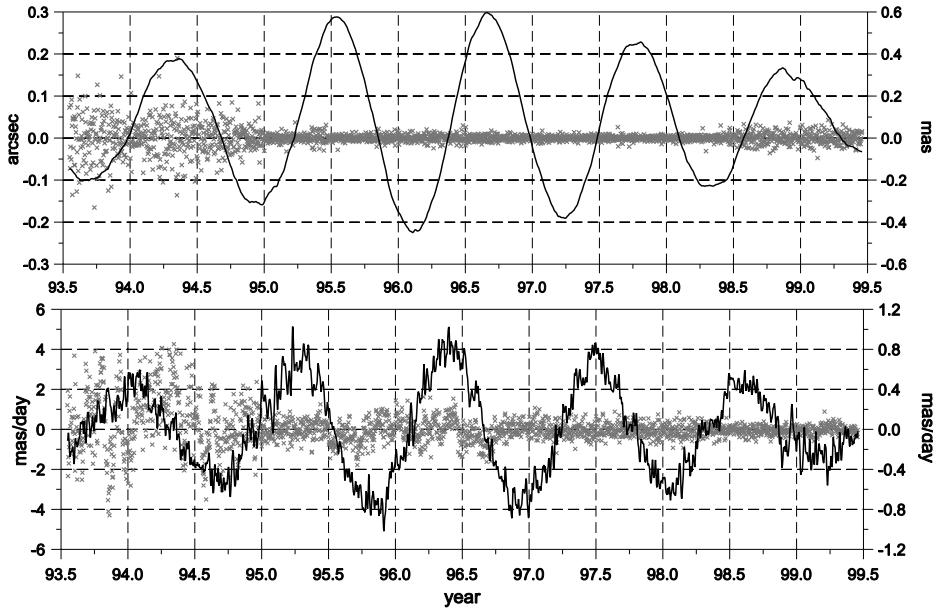


Fig. 10. Combined smoothing of pole coordinate x and its rate measured by GPS, using $\varepsilon = 100 \text{ day}^{-6}$, $\bar{\varepsilon} = 20 \text{ day}^{-4}$. Smoothed curves are shown as full lines and residuals (enlarged scale on the right) as grey crosses. Coordinate x is displayed in top, its rate in bottom

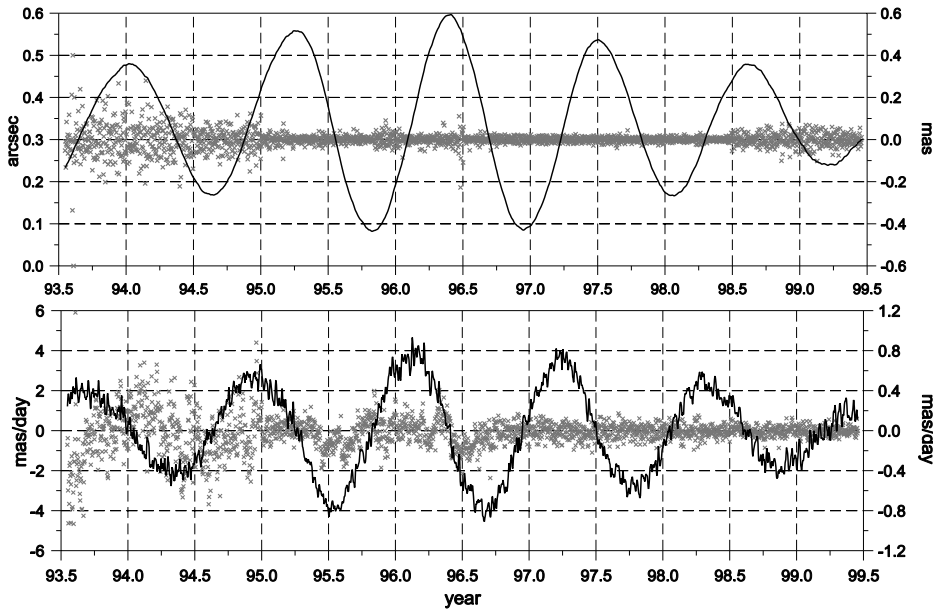


Fig. 11. Combined smoothing of pole coordinate y and its rate measured by GPS, using $\varepsilon = 100 \text{ day}^{-6}$, $\bar{\varepsilon} = 20 \text{ day}^{-4}$. Smoothed curves are shown as full lines and residuals (enlarged scale on the right) as grey crosses. Coordinate y is displayed in top, its rate in bottom

University of Berne provides not only the instantaneous coordinates of the pole but also their rate; both series are mutually independent in spite of the fact that they are based on the observations by the same technique – GPS. The data used in this study, covering roughly the interval 1993.5–1999.5, were subject to combined smoothing. The average a priori standard deviations of the series are respectively $23.4 \mu \text{ arcsec}$, $22.0 \mu \text{ arcsec}$ in x and y , and $18.6 \mu \text{ arcsec/day}$, $18.2 \mu \text{ arcsec/day}$ in their daily rates.

Although we made many tests, using solutions with different combinations of coefficients of smoothing, we were never able to find ε , $\bar{\varepsilon}$ that would lead to a posteriori values equal to average a priori values given above. It obviously reflects the fact that the formal standard deviations as reported by the analysis centers are so much underestimated that the observed function values and their first derivatives are not mutually compatible at the given level of accuracy.

Therefore we finally decided to use the same coefficients of smoothing as used in the last example of combining UT1 and lod, i.e. $\varepsilon = 100 \text{ day}^{-6}$, $\bar{\varepsilon} = 20 \text{ day}^{-4}$ whose transfer functions are shown in Fig. 8. They lead to approximately the same a posteriori standard deviations in x , y (respectively $20.0 \mu \text{ arcsec}$ and $20.9 \mu \text{ arcsec}$) but the standard deviations of their rates are significantly larger (respectively $96.1 \mu \text{ arcsec per day}$ and $99.1 \mu \text{ arcsec per day}$). The results are depicted in Figs. 10 and 11.

It can be seen that the accuracy of GPS-determined polar motion and its rate substantially improved after 1995. The coefficients of smoothing applied seem to be well chosen to suppress the noise of the observations, without affecting the real signal in the data. The combination of both types of observables (although not fully compatible on the level of their formal standard deviations), helps improve the solution.

4. Conclusions

The new method of combined smoothing further widens the possibilities of the original smoothing proposed by one of us three decades ago; it namely enables to combine Earth orientation parameters obtained by different space techniques, as demonstrated in the present paper. The tests made here show that it is advisable to use always such coefficients of smoothing ε , $\bar{\varepsilon}$ that yield approximately the same transfer functions (no matter whether leading to weak or strong smoothing). Otherwise (i.e., if much weaker smoothing is applied for first derivatives) one can easily obtain spurious peaks in the resulting series.

The practical examples of combining data from different techniques presented above show that the formal standard deviations of the results provided by analysis centers often do not reflect the real accuracy that is typically much lower, due to systematic effects.

The use of the proposed method is not strictly limited only to the problems demonstrated here – it can be as well used whenever we have independent measurements of a function of time (analytically not expressible) and its first derivatives. E.g., the method can be used to combine the comparisons of different atomic clocks with the comparisons of their frequencies. The code of the subroutine in Fortran and C++ is available on request from the authors.

Acknowledgements. This work has been supported by grant No. 205/98/1104 awarded by the *Grant Agency of the Czech Republic*. Its major part was developed during the first author's stay at Observatoire de Paris (IERS/CB and CNRS/URA8630) in May/June 1999.

References

- Čepek A., Vondrák J., 2000, *Acta Polytechn.* (in press)
 Erisman A.M., Tinney W.F., 1975, *Comm. ACM* 18, 177
 Feissel M., Lewandowski W., 1984, *Bull. Géod.* 58, 464
 Guinot B., 1988, *A&A* 192, 370
 Harmanec P., Horn J., Koubský P., et al., 1978, *Bull. Astron. Inst. Czechosl.* 29, 278
 Huang K.Y., Zhou X., 1981, *Acta Astron. Sin.* 22, 120
 Huang K.Y., Zhou X., 1982, *Acta Astron. Sin.* 23, 280
 Štefl S., 1995, *A&A* 294, 135
 Vondrák J., 1969, *Bull. Astron. Inst. Czechosl.* 20, 349
 Vondrák J., 1977, *Bull. Astron. Inst. Czechosl.* 28, 84
 Vondrák J., Gambis D., 2000, *Accuracy of Earth Orientation Parameters Series Obtained by Different Techniques in Different Frequency Windows*, in: Soffel M., Capitaine N. (eds.), *Journées 1999 Systèmes de Référence Spatio-temporels*, Observatoire de Paris, p. 206
 Whittaker E., Robinson G., 1946, *The Calculus of Observations* (4th ed.). Blackie & Son Ltd., London, p. 303
 Yoder C.F., Williams J.G., Parke M.E., 1981, *J. Geophys. Res.* 86, 881